Journal of Neonatal Surgery
ISSN(Online): 2226-0439
Vol. 14, Issue 32s (2025)
https://www.jneonatalsurg.com

OPEN ACCESS

Hippocampal Volume Analysis in Alzheimer's Disease

Deepeesh Vijayan*[1], Durai Saravanan[2]

[1]Department of Radio Diagnosis, Jawaharlal Institute of Postgraduate Medical Education & Research, Puducherry-605006, India.

[1]School of Science and Humanities (Life Sciences), Sathyabama Institute of Science and Technology, Chennai-600119, Tamil Nadu, India.

[2]Centre For Laboratory Animal Technology and Research, Sathyabama Institute of Science and Technology, Chennai-600119, Tamil Nadu, India.

Email ID: deepeesh098@gmail.com, Email ID: snegamsaran@gmail.com

*Corresponding author:

Email ID: deepeesh098@gmail.com

Cite this paper as: Deepeesh Vijayan, Durai Saravanan, (2025) Hippocampal Volume Analysis in Alzheimer's Disease. *Journal of Neonatal Surgery*, 14 (32s), 1189-1198.

ABSTRACT

Hippocampal volume change over time, as evaluated by MRI, offers excellent potential as a marker for Alzheimer's "disease. In this study, we consider, using publicly available Statistical Parametric Mapping (SPM) software, a fully automated and computationally efficient processing pipeline for atlas-based hippocampal volumetry in 75 amnestic subjects with mild cognitive impairment (MCI) from the Alzheimer's Disease Neuroimaging Initiative (ADNI). Subjects were split into two groups: MCI stable and MCI to probable Alzheimer's disease (AD) converters, based on follow-up diagnoses at 0, 6, and 12 months. From the baseline T1-weighted MRI, the hippocampal grey matter volume (HGMV) was measured and adjusted for age and total intracranial volume. The average processing time per subject on a typical PC was less than 4 minutes. To identify MCI to likely AD converters, the area under the receiver operator characteristic curves of the corrected hippocampal grey matter volume right (HGMVR) and hippocampal grey matter volume left (HGMVL) were determined. Using one-way ANOVA data on the MMSE score, HGMVR, and HGMVL, a ROC CURVE is computed to compare the control group versus MCI and the control group versus AD.

Keywords: *Alzheimer's Disease, Hippocampus Volumetry, Fully Automated, Mild Cognitive Impairment, Magnetic Resonance Imaging.*

1. INTRODUCTION

Alzheimer's disease (AD) is the leading cause of dementia and a significant health concern worldwide, affecting 20% of the population over the age of 80 [1]. Neuropathological evaluation of AD shows diffuse brain shrinkage and "specific changes in cortical cell clusters" [2]. Global cognitive impairment is a progressive illness known as dementia. It was estimated that about 35 million people globally had dementia in 2010. According to reports, some individuals with mild cognitive impairment (MCI) remain stable or regain full function, while others go on to develop dementia. [3, 4]. Therefore, one of the main objectives in public health is the development of biomarkers that can accurately signal the presence of the disease at an early stage. Alzheimer's disease is linked, macroscopically, to a progressive loss of brain tissue [5], which MRI may partially visualize in vivo without intrusive methods [6]. Unsurprisingly, MRI has garnered a lot of attention as a method to find biomarkers for Alzheimer's disease. Due to the lack of readily available software tools, MRI-based hippocampus volumetry has not yet been included in standard clinical diagnostic patient care." To ascertain if personal expertise mediated the connections between the amygdala and anterior hippocampal volume and perceived discrimination, Rosario et al. [7] conducted a study. Researchers analyzed T1-weighted images to obtain bilateral volumes from the hippocampus and amygdala using FreeSurfer 7.1.0. The usual and limbic-predominant hypometabolic subtypes of AD were the focus of Levin et al. [8] investigation of the connection between CR and these subtypes. We examined data from patients in the ADNI and ADNIGO/2 stages, including 174 AD dementia, 221 prodromal AD, and 59 Aβ-positive cognitively normal (CN). As a result, more sophisticated imaging techniques have lately been used to find helpful AD markers. While some research examined the brain as a whole [9–13], others [14–16] preferred to examine particular brain regions. Since the hippocampus

plays a significant role, it is aimed to investigate the adoption of the Hippocampal Unified Multi-Atlas Network as a particular hippocampal segmentation technique [17].

The AD biomarker study is notable for its groundbreaking work, especially the ADNI, a vast and comprehensive collection of open-source genomes, neuroimaging (positron emission tomography and MRI), and cognitive, behavioural, and clinical data. Specifically, the most recent phase of ADNI-3, which began in 2016 and is still in progress, has brought in updated MRI technologies [18], which are currently being partially studied in the literature. To compare static, structural, and dynamic functional aspects of the brain from resting-state functional MRI (fMRI) and structural magnetic resonance imaging (sMRI) between non-converters (MCI_NC) and MCI converters (MCI_C), Chen et al. [19] proposed a novel framework for inter-cohort MCI conversion prediction. Support vector machines were used to construct prediction models.

2. MATERIALS AND METHODS

Mild cognitive impairment (MCI) and Alzheimer's Disease (AD) are three approaches "to clinical imaging research that can be used in the long-term, multisite ADNI. ADNI data is accessible to the general public via http://adni.loni.usc.edu. Further details on the ADNI's inclusion and exclusion standards are at (http://adni.loni.ucla.edu/wp-content/uploads/2010/09/ADNI_GeneralProceduresManual.pdf). In 2003, the Food and Drug Administration (FDA), the National Institute on Ageing (NIA), private pharmaceutical companies, the National Institute of Biomedical Imaging and Bioengineering (NIBIB), and non-profit organisations established ADNI. Under the direction of Principal Investigator Michael W. Weiner, MD, the ADNI began operations in 2003 as a public-private partnership. The main objective of ADNI has been to determine whether the course of MCI and early AD may be measured with a combination of neuropsychological and clinical testing, serial magnetic resonance imaging (MRI), and biological markers.

Every participant provided written informed consent, and each institution's regional ethical committees authorized the study. The ADNI research design is a non-randomized, natural history, non-treatment study in which the participants were solely utilised to identify imaging biomarkers. Neuropsychological data and MRI images were downloaded from the ADNI database for this project. Seventy-five participants' additional data and magnetization-prepared rapid gradient echo (MPRAGE) pictures were gathered. The three groups of subjects were 25 with mild cognitive impairment (MCI), 25 with Alzheimer's disease (AD), and 25 individuals with cognitively normal (CN). Additionally, more demographic information was taken from the ADNI website. The Alzheimer's Disease Neuroimaging Initiative (ADNI) database provided the data. The ADNI results from the combined efforts of many coinvestigators from various academic institutions and corporate companies. Participants were gathered from more than 50 locations in the United States and Canada. We found and downloaded 75 datasets from the ADNI1 database. A screening 1.5 T MRI was required for inclusion, and subjects had to be diagnosed with MCI at enrolment and have follow-up diagnoses" at 0, 6, and 12 months.

ADNI-MCIs who were initially diagnosed with AD but were later reclassified as MCI were not included. 75 ADNI-MCIs in all were qualified: 75 ADNI-MCIs converted to AD during this time, and 103 ADNI-MCIs stayed steady for over 0 months. At the six-month follow-up exam, 25 MCI-to-AD converters were converted, 75 subjects were converted between the six- and twelve-month examinations and 25 subjects were converted between the six- and twelve-month exams. This paper also used the dataset obtained from the ADNI (http://adni.loni.usc.edu)database, available from October 31, 2016. The clinical, imaging markers and biochemical data with their statistical measurements are collected in a large number

2.1. Image analysis

Every subject's DICOM (Digital Information and Communication in Medicine) images were downloaded. Using the "dcm2niigui" utility in the MRIcron software, the downloaded DICOM images were converted to the NIfTI (Neuroimaging Informatics Technology Initiative)—FSL 4D NIfTI format. The present study uses a MATLAB code termed "HV," which is based on estimating hippocampus volume using 4D Nifti format and is fully integrated into the SPM GUI. The 'HV' toolbox can be used to segment hippocampus volume.

The retrieved values from various ROIs of the CN, MCI, and AD cohorts were compared based on a statistical comparison of segmented hippocampal volume using the SPSS tool (Statistical Tool for Social Sciences). The overall image processing involves segmenting the hippocampal in 3 different stages. The intensity values of the MRI images are normalized between 0 and 1, which provides uniform image color to do segments quickly and accurately. Then, the bias field is removed. Pearson's correlation is calculated between the test image and the trained image of brain MRI, and the optimal releases are selected. It is used as the machine learning processes can use the discovered knowledge. The statistical features are calculated, and textural features are extracted to decide the HV.

2.2. MRI acquisition and pre-processing

All ADNI1 participants for whom a screening 1.5T MRI was downloadable and recorded as normal for an entire year following the baseline clinical assessment served as the control group. As a consequence, 75 subjects were included. For the controls, there were no additional exclusion or inclusion criteria. There was no selection based on gender or age. A detailed description of the MR acquisition procedure utilized on the ADNI participants has been provided. Briefly, 1.5T systems were

used for MR imaging, and acquisition techniques were tailored to image-specific properties on various platforms. Using a sagittal magnetisation-prepared rapid gradient echo (MPRAGE) sequence with an approximation, high-resolution T1-weighted MRI images were obtained. Each individual underwent a 1.5T MRI. A "standardized MRI protocol (http://www.loni.ucla.edu/ ADNI/Research/Cores/index.html) was used to collect the data at several ADNI sites. This methodology was designed following a significant effort to evaluate and compare 3D T1-weighted sequences for morphometric analyses [20].

2.3 Estimation of Hippocampal Volume

One control point is located at the head of the hippocampus, one at the tail, and four points are placed manually on each of five equally spaced image slices that align with the ipsilateral hippocampal long axis at a perpendicular (i.e., at the inferior, superior, lateral and medial boundaries) to serve as rough local landmarks for hippocampal segmentation and to guide the initial transformations. To activate the hippocampus on the other side, repeat the final step. The iterative fluid transformation image matching technique then does automatic hippocampus segmentation using the landmarks as initial guidance. Hsu et al. [21] validated the approach for measuring hippocampus volume in senior adults, including those with AD and MCI. The normalized and modulated GM component image for each hippocampus was multiplied by a predetermined binary mask from a freely accessible toolbox to determine the hippocampal grey mass (HGMV) [22].

2.4 Statistical Analysis

ANOVA was used to compare more than two groups regarding age, Mini-Mental State Examination (MMSE) score, and TIV. If a significant effect was found, the heteroscedastic or homoscedastic unpaired two-sample t-test was used for post-hoc analyses between groups based on the outcome of Levene's test for equality of variance. The performance metric employed was the area (AUC) under the ROC curve. The Youden index, J = sensitivity + specificity - 1, is symmetric in specificity and sensitivity, so false positive and false negative classifications incur the same penalty. Cut-off values for HGMVad's specificity, sensitivity, accuracy, and predictive values were established by maximizing this index [23]. The danger of duplicate training samples limits the amount of variance that can be used to gauge the mistakes of accuracy estimations over cross-validation cycles. Accuracy measurements estimate the 95% confidence interval of [24]. We first restricted the analysis to patients with moderate cognitive impairment, typically the group with the most completed scans at each site," to lessen the impact of group heterogeneity between centres. Secondly, we increased bootstrapping using permutation testing.

SPM is a software used to learn and predict the internal changes in the brain cell or tissue images captured through various imaging modalities such as MRI, CT, X-ray, PET, etc. The systematic flow of the Statistical parametric Map tool or software used in processing the input brain MRI images is shown in Figure-1. As shown in Figure-1, the first step of SPM is to transform the input time-series brain image by realigning the raw image. Second, using the kernel, the artefacts in the images are removed, and the realigned image is smoothed. This realigned image is further normalized using the image normalization technique. Third, a general linear model is applied to design a matrix for the input MRI image. Based on this designed matrix result, the statistical parametric map result of the input MRI image is evaluated. It is performed based on Gaussian field theory. Once the SPM value is evaluated, the final prediction result is detected.

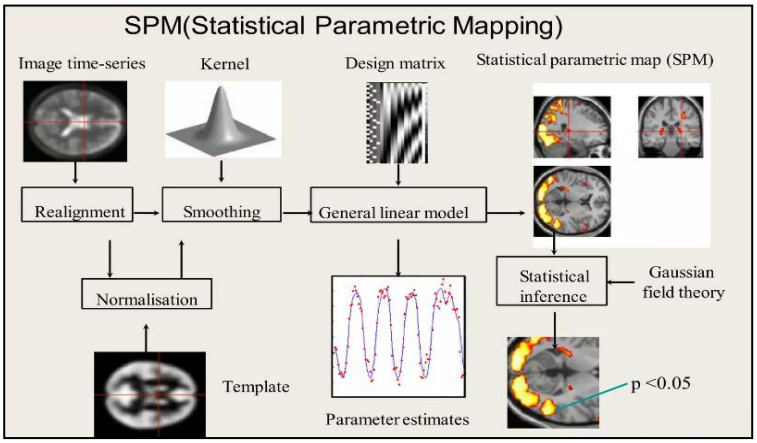

Figure-1. MRI Brain Image Processing Flow In SPM

3. EXPERIMENTAL RESULTS

There was no difference between the three categories of ADNI-MCI converters (between 0, 6,12 months) and stable ADNIMCIs. Compared to all three ADNI-MCI converter groupings, the stable ADNI-MCIs had a higher baseline MMSE

score. Regarding baseline MMSE, there was no difference between the converter subgroups. Table-1 presents the descriptive data of HGMVL and HGMVR. As expected, the hippocampal volumes of patients with Alzheimer's disease were smaller than those of people with MCI ($P < 0.0001$), and both groups' sizes were less than those among normal participants ($P < 0.0001$). In every group, there was a significant correlation between ($P < 0.01$) age with smaller baseline volumes. For the control group, the HGMVL mean ± Standard deviation is 4.340±0.5226, the MCI is 3.637±0.6468, and the AD is 3.347±0.6328. In a similar vein, the HGMVR for AD is 3.476±0.6136, MCI is 3.667±0.8336, and for control, it is 4.343±0.6013. The HGMVL's lower and upper 95% Confidence Intervals (CI) are 4.124±4.556 for control, 3.370±3.904 for MCI, and 3.286±3.608 for AD. The HGMVR's lower and upper 95% Confidence Intervals (CI) for control, MCI, and AD are, respectively, 4.095±4.591, 3.323±4.011, and 3.223±3.729.

Table 1. Descriptive statistics of HGMVL and HGMVR

	HGMVL			HGMVR		
	Control	**MCI**	**AD**	**Control**	**MCI**	**AD**
Number of values	25	25	25	25	25	25
Minimum	3.215	2.232	1.994	3.153	1.987	1.936
25% Percentile	4.003	3.106	2.945	4.023	2.969	3.096
Median	4.346	3.710	3.391	4.295	3.914	3.480
75% Percentile	4.672	4.116	3.814	4.742	4.405	3.949
Maximum	5.365	4.701	4.267	5.610	4.861	4.473
Mean	4.340	3.637	3.347	4.343	3.667	3.476
Std. Deviation	0.5226	0.6468	0.6328	0.6013	0.8336	0.6136
Std. Error of Mean	0.1045	0.1294	0.1266	0.1203	0.1667	0.1227
Lower 95% CI	4.124	3.370	3.086	4.095	3.323	3.223
Upper 95% CI	4.556	3.904	3.608	4.591	4.011	3.729

This paper focuses on explaining the assessment procedure for MRI in detecting the state of AD and its progression. Significant atrophy, particularly for AD, is detected using voxel-based morphometry. A stand-alone SPM software tool is used for AD detection globally. The structural analysis of AD is examined and evaluated using statistical information extracted from the MRI images. The output obtained from the experiment concerning predicting AD in MRI images is shown in Figure-2. Figure-2(a), (b), and (c) depict the results obtained from the experiment of the proposed model on predicting Alzheimer's disease from the input raw brain image. In Figure-2(a), among 256 slices, 129 slices detected the diseases; the detected portion of the brain is depicted at a coronal angle. Figure-2(b) evaluated 240 slices, of which 112 have diseases; the coronal view of the detected brain sample is clearly shown in Figure-2(b). Similarly, Figure-2(c) depicts the analysis result of the proposed evaluation of 256 slices. Of that, 125 are detected with Alzheimer's; the detection portion with the coronal view of the brain image is clearly shown in Figure-2(c).

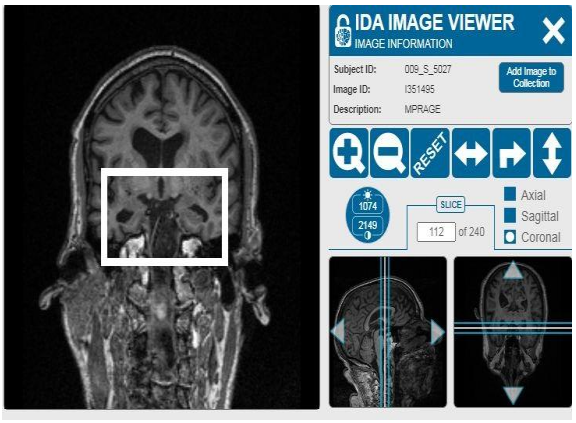

(a)

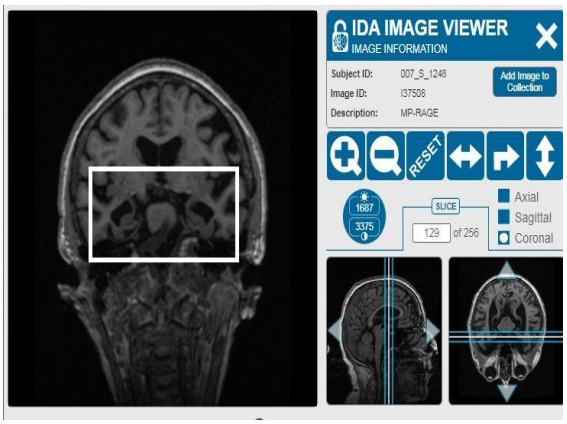

(b)

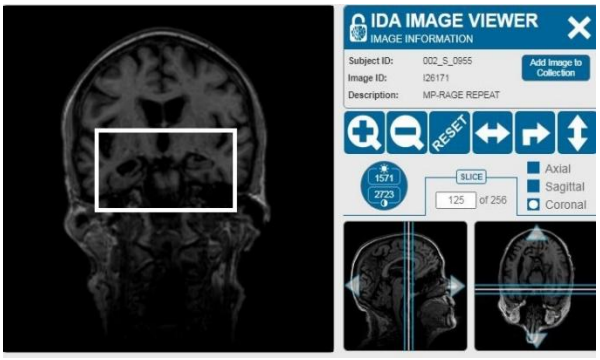

(c)

Figure-2. Input Sample Image Vs. AD Predicted Brain Image

Table-2 provides the number of measurements recorded from each patient using different markers, offering a comprehensive overview of the data collected for the study. The brain images were collected from the ADNI dataset (http://adni.loni.usc.edu/) and prepared on October 31st, 2016. This dataset includes various longitudinally covered biochemical, clinical, and imaging markers collected from each patient with different levels. The obtained observation result is shown in the table, which depicts the number of measurements analyzed based on different markers from each patient. The analysis result in Table-2 shows that HV has been recorded with a higher measurement rate among various markers than structural MRI, CSF, PET, and others. Following this, Florbetapir (AV45) and Fluoro-2-deoxy-D-glucose (FDG) markers have been recorded with high values over 24-to-28-month visits. Compared to volumetric measurements, the $A\beta_{42}$ and total-tau (t-tau) is highly observed but has less value through annual collection. The changes in the markers are analyzed through continuous iterations.

Table-2. Measurements of Individual Patients

	Number of measurements per individual						
	0	1	2	3	4	5+	Mean (SD)
HV	53	186	195	253	347	696	3.93 (2.00)
FDG	328	587	468	44	86	217	1.93 (1.92)
AV45	642	384	416	276	12	0	1.21 (1.13)
PIB	1,627	21	46	35	1	0	0.13 (0.54)
$A\beta_{42}$	308	1,235	39	63	44	41	0.57 (1.17)
t-tau	328	1,213	39	69	42	39	0.55 (1.16)

3.1 ROC curve

A lab test was performed on controls and patients. Two columns define these two groups. Unlike many statistics programs, Prism does not use a grouping variable. Instead, the groups are defined by columns. The values in each row are not paired in any way. Also, note that the sample sizes are unequal, which is fine. The proposed work aims to choose a cutoff value that separates 'normal' from 'abnormal' test results. To help make the decision, plot the tradeoff of sensitivity vs. specificity as a Receiver Operator Characteristic (ROC) curve. The ROC curve based on the MMSE score is presented in Table 3. The 95% CI for the control vs. MCI and control vs. AD reveals 0.7420 to 0.9508 and 0.9530 to 1.000, respectively. Both the control vs. MCI and the control vs. AD comparisons are statistically significant ($P < 0.0001$). The ROC curve for the MMSE score based on 100% specificity to sensitivity is shown in Figure-2 for control vs. MCI and control vs. AD using one-way analysis of variance (ANOVA) data.

Table-3. ROC CURVE based on MMSE Score

The area under the ROC curve	Control vs MCI	Control vs AD
Area	0.8464	0.9816
Std. Error	0.05326	0.01458
95% confidence interval	0.7420 to 0.9508	0.9530 to 1.000
P value	<0.0001	<0.0001
Data		
Controls	25	25
Patients (MCI)	25	25
Missing Patients	0	0
Missing Controls	0	0

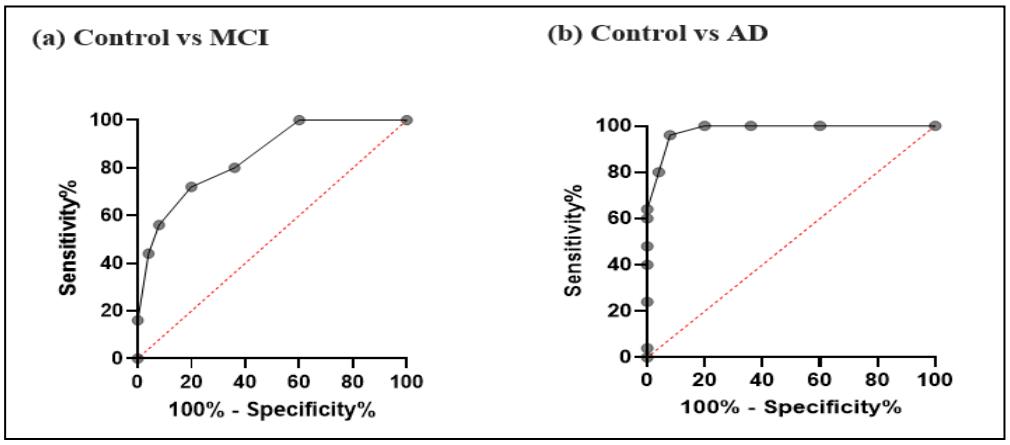

Figure-2. ROC CURVE based on MMSE score by one-way ANOVA data (a) Control vs MCI (b) Control vs AD

Table-4. ROC CURVE based on HGMVL

The area under the ROC curve	Control vs MCI	Control vs AD
Area	0.8064	0.8928
Std. Error	0.06032	0.04432
95% confidence interval	0.6882 to 0.9246	0.8059 to 0.9797
P value	0.0002	<0.0001
Data		
Controls	25	25
Patients (MCI)	25	25
Missing Patients	0	0
Missing Controls	0	0

Table-4 shows the ROC curve based on HGMVL with the 95% CI for control vs. MCI, which is 0.6882 to 0.9246, and for control vs AD, which is 0.8259 to 0.9797. The p-value shows significance for control vs MCI as $p = 0.0002$ and highly significant for control vs AD as $p < 0.0001$. Figure 3 displays the ROC curve based on 100% specificity to sensitivity for HGMVL, calculated using one-way ANOVA data for Control vs. MCI and Control vs. AD.\

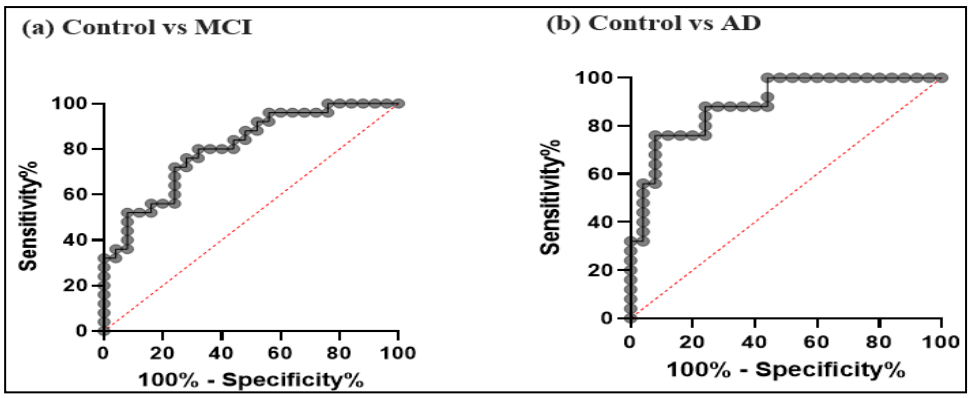

Figure 3. ROC CURVE based on HGMVL by one-way ANOVA data (a) Control vs MCI (b) Control vs AD

Table 5. ROC CURVE based on HGMVR

The area under the ROC curve	Control vs MCI	Control vs AD
Area	0.7232	0.8432
Std. Error	0.07146	0.05462
95% confidence interval	0.5831 to 0.8633	0.7362 to 0.9502
P value	0.0068	<0.0001
Data		
Controls	25	25
Patients (MCI)	25	25
Missing Patients	0	0
Missing Controls	0	0

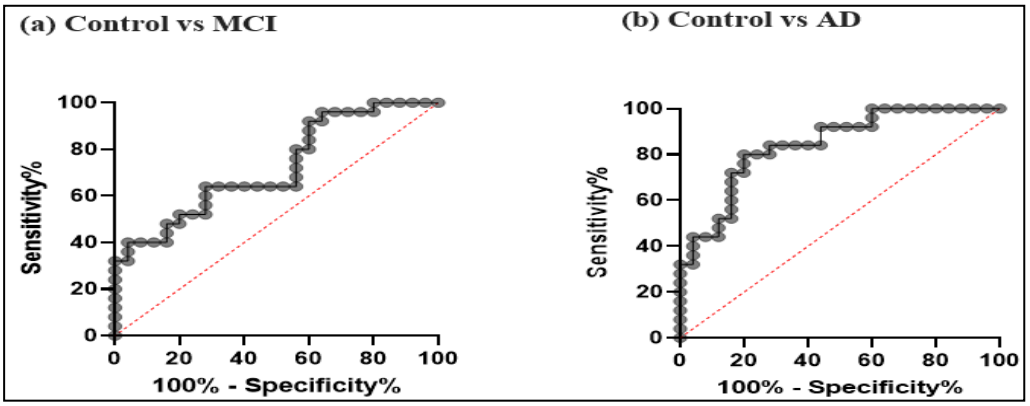

Figure 4. ROC CURVE based on HGMVR by one-way ANOVA data (a) Control vs MCI (b) Control vs AD

The hippocampal regions on the right (HGMVR) and left (HGMVL) of the Control, MIC, and AD patients. A black dot and triangles on each bar indicate the median and 95% confidence interval. The plots on the correct display the associated ROC curves and area under the curves (AUC). To determine if the mean of the difference between AUC_L and AUC_R was consistent with zero, the one-way ANOVA test was employed. Table 5 displays the HGMVR-based ROC curve, with 95% confidence intervals (CI) of 0.5831 to 0.8633 for control versus MCI and 0.7362 to 0.9502 for control versus AD. The control vs. MCI, p-value is significant at $p = 0.0068$, while the control vs. AD p-value is exceptionally significant at $p < 0.0001$. Figure-4 shows the ROC curve for HGMVR based on 100% specificity to sensitivity for Control vs. MCI and Control vs. AD using one-way ANOVA data.

4. DISCUSSION

Although the left side of the hippocampal formation appears to play a major role, as explained in [25, 26], the left side is typically smaller, and the accuracy of AD prediction is not as strongly correlated with laterality. Our results are consistent with a meta-analysis combining information from multiple research projects, which indicates that hippocampal atrophy on the left is typically more severe than on the right [27] and with [28], which found that in MCI and AD, the left hemisphere saw a much lower volume loss than the right.

The purpose of this study is not to speculate on the importance of laterality in AD prediction. However, significant physiological discoveries exist connecting hippocampus laterality with putative neurodegenerative processes. Hippocampal volumes are obtained with a 3% precision using the "Hippocampal Unified Multi-Atlas Network (HUMAN) segmentation method; volume measurements successfully detect AD, with an area under the curve (AUC) of AUC1 = 0.08 ± 0.02. AUC2 = 0.76 ± 0.05 indicates that segmented volumes can also show the more modest effects seen in MCI participants. In the long run, the algorithm remains consistent and repeatable, even for 24-month follow-up scans [29].

An algorithm for segmenting hippocampi was published by Chincarini et al. [30] and validated using the gold-standard manual tracing database. ADNI participants divided 460 into groups and scanned each subject twice: once at baseline and once at the 12- and 24-month follow-up points (1.5T, T1 MRI). The reference cohorts are Mild Cognitive Impairment vs CTRL, subsequently developed into AD dementia (MCI-co/CTRL) and AD/CTRL. The bilateral age-corrected annualized atrophy rate (%/year) for CTRL was -1.6 (0.6); for MCI-nc, it was -2.2 (1.0); for MCI-co, it was -3.2 (1.2), and for AD it was -4.0 (1.5). The area under the ROC curve (AUC) = 0.88 for CTRL vs. MCI-co and AUC = 0.93 for CTRL vs. AD were obtained from the combined. (v, Λ) discrimination ability.

Our findings show that the rigorous techniques of the ADNI can be used to successfully regulate site-to-site variability in MRI for studies of hippocampus rates. The outcome is significant since major research, such as clinical trials involving 75 participants, needs the utilization of several MRI facility settings. We were especially curious to compare the capacities of multisite and single-site investigations to determine a specific atrophy rate because, as is common in investigational study designs," additional variability is inherently introduced in many MRI site settings compared to a single-site setting. Lastly, hippocampus atrophy over 6 months and accelerated atrophy over 12 months in Alzheimer's disease patients with mild cognitive impairment demonstrate the capability of magnetic resonance imaging (MRI) to monitor morphological brain changes through time in an enormous multisite setting.

5. CONCLUSION

The current study suggests an SPM8-based processing pipeline for fully automated hippocampus volumetry, which performs comparably to more sophisticated methods for predicting MCI-to-AD conversion. The processing pipeline runs close to real-time and is entirely based on open-source software. The area under the receiver operator characteristic curves of the corrected HGMVR and HGMVL were calculated to identify MCI to probable AD converters. A ROC CURVE is generated based on 100% specificity to sensitivity to compare the control group against MCI and the control group against AD using one-way ANOVA data on the MMSE score, HGMVR, and HGMVL. Regardless of conversion status, neurodegeneration rates were higher in MCI patients. In addition, those with positive MCI demonstrated a roughly two-fold higher chance of developing AD, regardless of the impact of degeneration rate on conversion. This may make integrating hippocampus volumetry into standard clinical diagnostic treatment easier in patients with cognitive impairment.

Acknowledgement

We sincerely thank Dr. R. Sivaprakasam, Assistant Professor, Centre for Brain Research, Indian Institute of Science Campus, CV Raman Avenue, Bangalore 560012. India for providing us with the Brain Samples as mentioned in this study for our research.

REFERENCES

[1] Ferri CP, Prince M, Brayne C, Brodaty H, Fratiglioni L, Ganguli M, et al. Global prevalence of dementia: a Delphi consensus study. Lancet 2005; 366: 2112–7.

[2] Soria Lopez JA, González HM, Léger GC. Alzheimer's disease. Handb Clin Neurol. 2019;167:231–55.

[3] Delgado-Alvarado M, Gago B, Navalpotro-Gomez I, et al. Biomarkers for dementia and mild cognitive impairment in Parkinson's disease. Mov Disord Off J Mov Disord Soc. 2016;31:861–81.

[4] Morley JE. An overview of cognitive impairment. Clin Geriatr Med. 2018;34:505–13.entia: a Delphi consensus study. Lancet 2005; 366: 2112–7.

[5] Braak H, Braak E. Evolution of neuronal changes in the course of Alzheimer's disease. J Neural Transm Suppl 1998; 53: 127–40.

[6] Thompson PM, Hayashi KM, Dutton RA, Chiang MC, Leow Alzheimer's disease, Sowell ER, et al. Tracking

Alzheimer's disease. Ann N Y Acad Sci 2007; 1097: 183–214.

[7] Rosario, M., Alotaibi, R., Espinal-Martinez, A. O., Ayoub, A., Baumann, A., Clark, U., ... & Schon, K. (2024). Personal Mastery Attenuates the Association between Greater Perceived Discrimination and Lower Amygdala and Anterior Hippocampal Volume in a Diverse Sample of Older Adults. *bioRxiv*, 2024-01.

[8] Levin, F., Grothe, M. J., Dyrba, M., Franzmeier, N., Teipel, S. J., & Alzheimer's Disease Neuroimaging Initiative. (2024). Longitudinal trajectories of cognitive reserve in hypometabolic subtypes of Alzheimer's disease. *Neurobiology of Aging*, *135*, 26-38.

[9] Sluimer J, Vrenken H, Blankenstein M, Fox N, Scheltens P, Barkhof F, van der Flier W. Whole-brain atrophy rate in Alzheimer disease Identifying fast progressors. Neurology. 2008;70(19 Part 2): 1836–41.

[10] Amoroso N, Errico R, Bellotti R. PRISMA-CAD: a fully automated method for computer-aided diagnosis of dementia based on structural MRI data. In: Proc MICCAI workshop challenge on computer-aided diagnosis of dementia based on structural MRI data. 2014. pp. 16–23.

[11] Beheshti I, Demirel H, Initiative ADN. Probability distribution function-based classification of structural MRI for detecting Alzheimer's disease. Comput Biol Med. 2015;64:208–16.

[12] Bron EE, Smits M, Van Der Flier WM, Vrenken H, Barkhof F, Scheltens P, Papma JM, Steketee RM, Orellana CM, Meijboom R. Standardized evaluation of algorithms for computer-aided diagnosis of dementia based on structural MRI: the CADDementia challenge. NeuroImage. 2015;111:562–79.

[13] Allen GI, Amoroso N, Anghel C, Balagurusamy V, Bare CJ, Beaton D, Bellotti R, Bennett DA, Boehme KL, Boutros PC. Crowdsourced estimation of cognitive decline and resilience in Alzheimer's disease. Alzheimer's Dement. 2016;12(6):645–53.

[14] Colliot O, Chételat G, Chupin M, Desgranges B, Magnin B, Benali H, Dubois B, Garnero L, Eustache F, Lehéricy S. Discrimination between Alzheimer disease, mild cognitive impairment, and normal aging by using automated segmentation of the Hippocampus 1. Radiology. 2008;248(1):194–201.

[15] Tangaro S, Amoroso N, Boccardi M, Bruno S, Chincarini A, Ferraro G, Frisoni G, Maglietta R, Redolf A, Rei L. Automated voxel-by-voxel tissue classification for hippocampal segmentation: methods and validation. Physica Medica. 2014;30(8):878–87.

[16] Poulin SP, Dautof R, Morris JC, Barrett LF, Dickerson BC, Initiative ADN. Amygdala atrophy is prominent in early Alzheimer's disease and relates to symptom severity. Psychiatry Res Neuroimag. 2011;194(1):7–13.

[17] Amoroso N, Errico R, Bruno S, Chincarini A, Garuccio E, Sensi F, Tangaro S, Tateo A, Bellotti R, Initiative ADN. Hippocampal unified multi-atlas network (HUMAN): protocol and scale validation of a novel segmentation tool. Phys Med Biol. 2015;60(22):8851.

[18] Michael W. Weiner, Dallas P. Veitch, Paul S. Aisen, Laurel A. Beckett, Nigel J. Cairns, Robert C. Green, Danielle Harvey, Clifford R. Jack Jr., William Jagust, John C. Morris, et al., The Alzheimer's Disease Neuroimaging Initiative 3: Continued innovation for clinical trial improvement, Alzheimer's Dementia 13 (5) (2017) 561–571.

[19] Chen, Z., Chen, K., Li, Y., Geng, D., Li, X., Liang, X., ... & Alzheimer's Disease Neuroimaging Initiative. (2024). Structural, static, and dynamic functional MRI predictors for converting mild cognitive impairment to Alzheimer's disease: Inter-cohort validation of Shanghai Memory Study and ADNI. *Human Brain Mapping*.

[20] Jack CR Jr, Bernstein MA, Fox NC, Thompson P, Alexander G, Harvey D, et al. The Alzheimer's Disease Neuroimaging Initiative (ADNI): MRI methods. J Magn Reson Imaging 2008a; 27: 685–91.

[21] Hsu YY, Schuff N, Du AT, Mark K, Zhu X, Hardin D, et al. Comparison of automated and manual MRI volumetry of hippocampus in normal aging and dementia. J Magn Reson Imaging 2002; 16: 305–10.

[22] Eickhoff SB, Stephan KE, Mohlberg H, Grefkes C, Fink GR, Amunts K, Zilles K (2005) A new SPM toolbox for combining probabilistic cytoarchitectonic maps and functional imaging data. Neuroimage 25, 1325-1335.

[23] Youden WJ (1950) Index for rating diagnostic tests. Cancer 3, 32-35.

[24] Kohavi R. (1995) A study of cross-validation and bootstrap for accuracy estimation and model selection. Proceedings of the 14th International Joint Conference on Artificial Intelligence (IJCAI), Montreal, Quebec, Canada, Vol. 2, pp. 1137-1143.

[25] Apostolova, L.G., Thompson, P.M., Green, A.E., Hwang, K.S., Zoumalan, C., Jack, C.R., Harvey, D.J., Petersen, R.C., Thal, L.J., Aisen, P.S., Toga, A.W., Cummings, J.L., DeCarli, C.S., 2010. 3D comparison of low, intermediate, and advanced hippocampal atrophy in MCI. Human Brain Mapping 31, 786–797. URL: http://doi.wiley.com/10.1002/hbm.20905, 666 doi:10.1002/hbm.20905.

[26] Okonkwo, O.C., Xu, G., Dowling, N.M., Bendlin, B.B., LaRue, A., Hermann, B.P., Koscik, R., Jonaitis, E.,

Rowley, H.a., Carlsson, C.M., Asthana, S., Sager, M.a., Johnson, S.C., 2012. A family history of Alzheimer's disease predicts hippocampal atrophy in healthy middle-aged adults. Neurology 78, 1769–1776. URL: http://www.neurology.org/cgi/doi/10.1212/WNL. 0b013e3182583047, doi:10.1212/WNL.0b013e3182583047

[27] Shi, F., Liu, B., Zhou, Y., Yu, C., Jiang, T., 2009. Hippocampal volume and asymmetry in mild cognitive impairment and Alzheimer's disease: Meta-analyses of MRI studies. Hippocampus 19, 1055–64. URL: http://www.ncbi.nlm.nih.gov/pubmed/19309039.

[28] Frank´o, E., Joly, Olivier, A.D.N.I., 2013. Evaluating Alzheimer's disease progression using the rate of regional hippocampal atrophy. PloS one 8, 737 e71354. URL: http://www.pubmedcentral.nih.gov/articlerender.fcgi?artid=3741167\&tool=pmcentrez\&rendertype=abstract, doi:10.1371/journal.pone.0071354.

[29] Amoroso, N., Rocca, M. L., Bellotti, R., Fanizzi, A., Monaco, A., Tangaro, S., & Alzheimer's Disease Neuroimaging Initiative Michael Weiner. (2018). Alzheimer's disease diagnosis based on the hippocampal unified multi-atlas network (HUMAN) algorithm. *Biomedical engineering online*, *17*, 1-16.

[30] Chincarini, A., Sensi, F., Rei, L., Gemme, G., Squarcia, S., Longo, R., ... & Alzheimer's Disease Neuroimaging Initiative. (2016). Integrating longitudinal information in hippocampal volume measurements for the early detection of Alzheimer's disease. *NeuroImage*, *125*, 834-847.